[Plant Signaling & Behavior 1:3, 122-133, May/June 2006]; ©2006 Landes Bioscience

Research Paper

Auxin Immunolocalization Implicates Vesicular Neurotransmitter-Like Mode of Polar Auxin Transport in Root Apices

Markus Schlicht[1]
Miroslav Strnad[2]
Michael J. Scanlon[3]
Stefano Mancuso[4,5]
Frank Hochholdinger[6]
Klaus Palme[7]
Dieter Volkmann[1]
Diedrik Menzel[1]
Frantisek Baluska[1,5,8,*]

[1]IZMB; Rheinische Friedrich-Wilhelms-Universität; Bonn, Germany

[2]Laboratory of Growth Regulators; Palacky University & Institute of Experimental Botany ASCR; Olomouc, Czech Republic

[3]Department of Botany; University of Georgia; Athens, Georgia USA

[4]Department of Horticulture; University of Florence; Florence, Italy

[5]International Plant Neurobiology Laboratory; Florence, Italy and Bonn, Germany

[6]University of Tuebingen; ZMBP—Center for Plant Molecular Biology; Department of General Genetics; Tuebingen, Germany

[7]University of Freiburg; Center for Applied Biosciences; Freiburg, Germany

[8]Institute of Botany; Slovak Academy of Sciences; Bratislava, Slovak Republic

*Correspondence to: Frantisek Baluska; Rheinische Friedrich-Wilhelms-Universität; Kirschallee 1; Bonn, D 53115 Germany; Tel.: +0049.228.734761; Fax: +0049.228.739004; Email: baluska @uni-bonn.de

Received 03/31/06; Accepted 04/03/06

Previously published online as a *Plant Signaling & Behavior* E-publication: http://www.landesbioscience.com/journals/psb/abstract.php?id=2759

KEY WORDS

actin, auxin, maize, secretion, vesicles, neurotransmitter

ACKNOWLEDGEMENTS

See page 131.

NOTE

Supplemental material can be found at: http://www.landesbioscience.com/journals/psb/supplement/schlichtPSB1-3-sup.pdf

ABSTRACT

Immunolocalization of auxin using a new specific antibody revealed, besides the expected diffuse cytoplasmic signal, enrichments of auxin at end-poles (cross-walls), within endosomes and within nuclei of those root apex cells which accumulate abundant F-actin at their end-poles. In Brefeldin A (BFA) treated roots, a strong auxin signal was scored within BFA-induced compartments of cells having abundant actin and auxin at their end-poles, as well as within adjacent endosomes, but not in other root cells. Importantly, several types of polar auxin transport (PAT) inhibitors exert similar inhibitory effects on endocytosis, vesicle recycling, and on the enrichments of F-actin at the end-poles. These findings indicate that auxin is transported across F-actin-enriched end-poles (synapses) via neurotransmitter-like secretion. This new concept finds genetic support from the *semaphore1*, *rum1* and *rum1/lrt1* mutants of maize which are impaired in PAT, endocytosis and vesicle recycling, as well as in recruitment of F-actin and auxin to the auxin transporting end-poles. Although PIN1 localizes abundantly to the end-poles, and they also fail to support the formation of in these mutants affected in PAT, auxin and F-actin are depleted from their end-poles which also fail to support formation of the large BFA-induced compartments.

INTRODUCTION

Polar transcellular auxin transport (PAT) is important for both growth regulation and control of polarity and pattern formation in plants.[1-5] In the last few years, there has been a dramatic increase in our knowledge on several proteins which are known to be involved in auxin transport, but we still lack information about how exactly auxin moves across cellular boundaries.[4-6] Rather unexpectedly, putative auxin transporters of the PIN family were shown to accomplish rapid vesicular recycling between the plasma membrane and endosomal compartments in *Arabidopsis*[7] and in maize[8] cells. There are three classes of inhibitors, differing chemically and in their action mechanisms, which prevent PAT along cell files of plant organs. These include TIBA, NPA and several morphactins all of which effectively inhibit PAT.[9,10] Unfortunately, it is still unknown how any of these PAT inhibitors act at the cellular level. Recent studies surprisingly revealed that TIBA and NPA act as unspecific inhibitors of endocytosis and vesicle recycling.[11,12] Here we confirm this feature also for morphactins.

Apparently unrelated to these classical inhibitors of PAT, auxin efflux from cells is also effectively and rapidly inhibited by two other inhibitors that block secretion from eukaryotic cells, monensin and brefeldin A (BFA).[12-15] For instance, the potent exocytosis inhibitor BFA blocks PAT within a few minutes and also leads to the formation of endosomal BFA compartments,[16] within which recycling molecules of the PAT machinery are entrapped together with cell wall pectins.[12,17] Importantly, although BFA inhibits PAT very rapidly,[12,14] nearly two hours of BFA treatment are necessary to remove most, but still not all, of the PIN molecules from the plasma membrane and to trap them within the BFA-induced endocytic compartments.[8,11,12,16] Similarly like cold treatment and depolymerization of the actin cytoskeleton,[7,11,16] TIBA and auxin treatments inhibited endocytosis to such an extent that larger BFA-induced compartments could not form in the TIBA/ auxin-BFA double treated cells.[7,11,12]

Up to now, all published auxin visualization procedures have drawbacks. First of all, auxin antibodies used in these previous studies are not monospecific. Secondly, the cross-linking agent, EDC, used to immobilize the small auxin molecules[3,18] has drastic effects on F-actin in cells of maize root apices (Suppl. Fig. 1). Thus, EDC might alter significantly the localization of other antigens too. In addition, although auxin responsive promoter

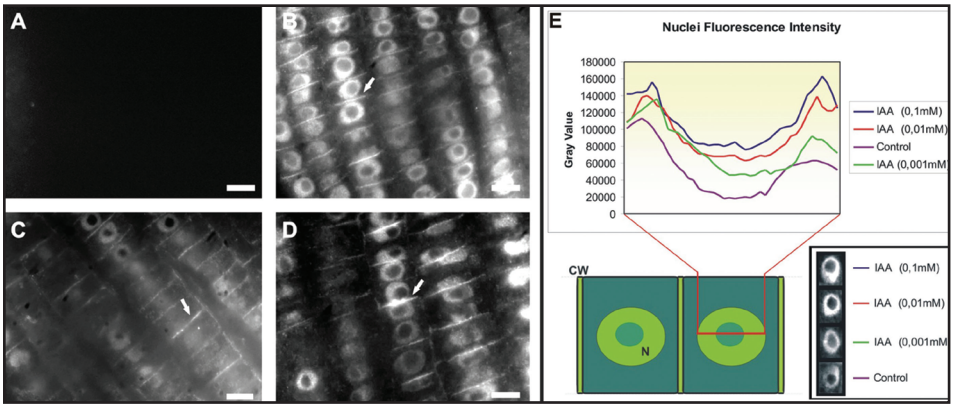

Figure 1. IAA labelings in maize root apices: antibody specificity. (A) Labeling with the IAA antibody immunodepleted with an excess of IAA for 24 h. (B) Labeling with the IAA antibody incubated with an excess of 2,4D for 24 h. (C) Labeling with the IAA antibody incubated with an excess of NAA for 24 h. (D) Labeling with the IAA antibody incubated with an excess of IBA for 24 h. White arrows indicate auxin-enriched end-poles. (E) Comparison of the fluorescence intensities of transition zone cells after treatments with different IAA concentrations. The medium intensities of transition zone cells of 5 roots per treatment are put into graphs. For the comparison, root sections labeled with the same antibody concentration were used. The pictures were recorded with the same exposure time. (CW, cell wall; N, nucleus). Bars: (B) 18 μM, (C) 12 μM, (D) 10 μM.

elements are perfect tools to visualize auxin signaling activities, they are less useful to localize both extra- and intra-cellular auxin as they only show the activity of these diverse auxin responsive promoters. So it is not surprising that the three most often used auxin-responsive promoters (DR5, BA3, GH3) show different, often contrasting, expression patterns. For instance, the DR5 reporter shows maximum activity in the root cap columella and quiescent centre cells,[19-21] whereas the BA3 has its maximum in root cells embarking on rapid cell elongation[22-24] (see also Suppl. Fig. 3). Moreover, these auxin-responsive promoter reporters are not absolutely specific for IAA. For example, the DR5-reporter is activated by brassinolides as well[25] and, in fact, it requires exposure to brassinolides to reach full activities.[26] Therefore, it is not entirely correct, though often practiced, if the DR5 reporter maximum is interpreted as a so-called 'auxin maximum', implying that it would correspond to the highest amount of free auxin in cells.[19-21,27]

BFA inhibits PAT rapidly,[14,15,28] due to a block in auxin efflux after some 10 minutes.[14,28] Importantly, wash-out of BFA restores auxin efflux also quite rapidly, within some 20 min.[28] How is it possible that such short treatments with a secretion inhibitor manipulates auxin efflux so rapidly? At these short exposure times, all the necessary proteins of the auxin efflux apparatus are still located at the plasma membrane as their plasma membrane presentation times are typically above ten minutes.[11,12,28] Currently, the most accepted model is that PIN proteins show their auxin efflux activity at the plasma membrane. Although this simple model is appealing, it is unable to explain the rapidity with which BFA inhibits polar transport of auxin.[14,15,28]

As a plausible alternative, a neurotransmitter-like secretory model has been proposed in which auxin is sequestered within endosomes via vesicular transporters and then might be secreted via a BFA-sensitive process out of the cells.[4,29,30] If PIN proteins had their activities at membranes delimiting vesicles and recycling endosomes,[29,31] they would enrich these vesicular compartments with IAA. Endosomes and recycling vesicles could fuse with the plasma membrane via a stimulus-activated BFA-sensitive process.[32] This would lead to a secretion of IAA out of cells in a quantal manner, resembling the process of synaptic vesicle secretion. A neurotransmitter-like nature of auxin transport could explain the fast inhibitory effects of BFA on PAT as well as the high PIN1 turnover at the plasma membrane. For this and other compelling reasons, we have recently introduced the term "plant synapse".[29,33] Our concept would also explain a second mystery[34] concerning *Arabidopsis* embryos, which generate a so-called auxin maximum at the emerging root pole as well as auxin gradients across the developing embryo.[3,20] This phenomenon is very difficult to explain by the classical version of the chemiosmotic theory, because it lacks any mechanisms that would restrict the free diffusion of auxin through the cytoplasm, as well as from cell-to-cell by the means of plant plasmodesmata connections.[34,35] The attractive feature of the neurotransmitter-like mode of auxin transport is that endosomes could both exclude auxin from the plasmodesmata orifices and transport it effectively towards those subcellular sites which are relevant for auxin signalling and transport. For instance towards the nuclei, or for the localized secretion in those cells which are part of the PAT pathway.

For auxin visualization on the cellular level, a specific antibody is the tool of choice. However, all auxin antibodies in use are not specific enough. Here we introduce a new highly specific auxin antibody, recognizing only IAA, which allows us to address critical questions with respect to auxin cell biology. We report here that IAA accumulates at the end-poles and adjacent endosomes only in those root cells which are active in transcellular transport of auxin.

MATERIALS AND METHODS

Plant material and inhibitor treatments. Maize grains (*Zea mays* L.), *Semaphore1, lrt1, rum1* and *lrt1-rum1* mutants were soaked for six hours and germinated in well moistened rolls of filter paper for four days in darkness at 20°C. Young seedlings with straight primary roots, either 50–70 mm long (wildtype, *lrt1* and *rum1*), or 25–60 mm (of the slower growing *Semaphore1* and *lrt1-rum1*) were selected for inhibitor treatments and subsequent immunolabeling studies. Unless stated otherwise, all chemicals were obtained from Sigma Chemicals (St. Louis, MO, USA). For pharmacological experiments, root apices were submerged into appropriate solutions at room temperature. For brefeldin A treatment, we used a 10^{-2} M stock solution (made in DMSO) further diluted in distilled water to achieve effective working solution of 10^{-4} M immediately before submergence of root apices for ten minutes or two hours. Latrunculin B, NPA, TIBA, Flurenol, Chlorflurenol, Chlorflurenolmethyl and IAA were used at 10^{-5} M for two hours.

Immunization schedule and purification of IAA-N-antibodies. The immunization schedule and purification of antibodies are described in details in previous papers.[70-72] The antibodies have been purified by ammonium sulphate precipitation. However, for the immunocytochemical labeling protein A[73] and IAA-N1-specific

Table 1 **Assay parameters of IAA-N-antibodies in ELISAs**

Antibody Characteristic in ELISA	Antibody No. 156
Titre	1:1250
Unspecific binding	3.5%
Midrange (B/Bo = 50%)	360 pmol
Detection limit	35 fmol, 8 ng
Linear range of measurement	22–5000 fmol
Intraassay variability	5.6%
Interassay variability	7.4%
Amount of tracer per assay	16.7 ng

affinity chromatography were also used, as described in more details previously.[37,38]

Characterization of antibodies by enzyme-linked immunosorbent assay. The IAA-N1-antibodies were characterized using a modification of the ELISA protocol described by Weiler et al.[74] The microtiter-plates (Gama, Ceské Budejovice, Czech Republic) were coated with 150 µl of rabbit antibodies (5 $\mu g.ml^{-1}$ 50 mM $NaHCO_3$, pH 9.6). The wells were washed with distilled water, filled with 200 µl of bovine serum albumin solution (0.04 $g.L^{-1}$) and incubated for 1 h at 25°C. After decanting and two washes with dist. H_2O the wells were filled in the following sequence: 50 µl TBS, 50 µl of standard or sample in TBS and 50 µl of IAA-alkaline phosphatase tracer diluted in TBS-bovine serum albumin buffer (0.04 $g.L^{-1}$). Non-specific binding was determined by adding an excess (200 pmol) of a standard; for maximum tracer binding, TBS was used instead of standard. After one minute shaking, the plates were incubated for one hour at 25°C. The decanted plates were then washed four times with TBS and filled immediately with 150 µl of a *p*-nitrophenylphosphate solution (1 $mg.ml^{-1}$ 50 mM $NaHCO_3$, pH 9.6). The reaction was stopped after one hour incubation at 25°C by adding 50 µl 3M KOH and the absorbance measured at 405 nm in a Titertek Multiscan MCC 340 (Flow Labs, Irvine, UK). Sigmoidal curves for standards and cross-reacting compounds were linearized by log-logit transformation as follows: logit B/Bo = ln (B/Bo)/(100-B/Bo).[74]

Indirect immunofluorescence labeling. Fixation consisted of excising of apical root segments (7 mm) encompassing the major growth zones into 3.7% formaldehyde prepared in stabilizing buffer (SB; 50 mM PIPES, 5 mM $MgSO_4$ and 5 mM EGTA, pH 6.9) for one hour at room temperature. Following rinsing in SB, the root apices were dehydrated in a graded ethanol series diluted with phosphate buffered saline (PBS). Then they were embedded in Steedman's wax and processed for immunofluorescence (for details see ref. 39). To enable efficient penetration of antibodies, sections were dewaxed in absolute ethanol, passed through a graded ethanol series diluted with PBS and then kept in PBS for 20 min. After that the sections were transferred to PBS containing 2% BSA for 15 min at room temperature.

They were then incubated with the following primary antibodies: JIM5 monoclonal antibodies diluted 1:20, anti-RGII polyclonal antibodies[16] diluted 1:100, anti-PIN1 polyclonal antibodies diluted 1:40, anti-IAA polyclonal antibodies diluted 1:20. All primary antibodies were diluted in PBS and the buffers were supplemented with 1% BSA. Sections were incubated in primary antibody for one hour at room temperature. After rinsing in PBS, the sections were incubated for one hour either with FITC/TRITC-conjugated anti-rat IgGs (JIM5), or with anti-rabbit IgGs (Actin, Auxin, PIN1, RGII), each raised in goat and diluted 1:100 in appropriate buffer containing 1% BSA. A further PBS rinse (ten minutes) preceded ten minutes treatment with 0.01% Toluidine Blue to diminished autofluorescence of root tissues. The sections were then mounted using an anti-fade mounting medium containing *p*-phenylenediamine[39] and examined with an Axiovert 405M inverted microscope (Zeiss, Oberkochen, Germany) equipped with epifluorescence and standard FITC excitation and barrier filters. Identical microscope settings were used to compare the labelings of different treatments.

Table 2 **Molar cross-reactivities of different auxins and related compounds with anti-IAA-N-antibodies**

Compound	Cross-Reactivity (%)
Indole-3-acetic acid	100
Indole-3-acetic acid methylester	0
Indole-3-acetone	0.22
Indole-3-propionic acid	0.27
Indole-3-butyric acid	0.06
Indole-3-acetaldehyde	0
Indole-3-ethanol	0
Indole-3-glyoxylic acid	0
Indole-3-acetonitrile	0.25
Indole-3-pyruvic acid	0
Indole-3-lactic acid	0
Indole-3-acrylic acid	0.11
Indole-3-aldehyde	0
Indole-3-acetamide	0
Indole-3-acetyalanine	0
Indole-3-acetylphenylalanine	0
Indole-3-acetylasparticacid	0
Indole-3-acetyltryptophan	0
Indole-3-acetylleucine	0
Indole-3-acetylvaline	0
5-hydroxyindole-3-acetic acid	0.93
α-naphtylacetic acid	5.75
2,4-dichlorophenoxyacetic acid	0.29
Tryptophan	0.09
Tryptamine	0

Double immunofluorescence labeling. After the labeling of the IAA with TRITC-conjugated anti-rabbit IgGs preceded a 45 min post fixation with 3.7% formaldehyde prepared in PBS, followed by a second blocking step with PBS containing 2% BSA for 15 min at room temperature. The labeling of PIN1 and JIM5 followed our standard protocol.

Sucrose density gradient, aqueous two-phase system and immunoblotting. Root tissue of four days treated or untreated maize was collected and grinded in TE-buffer: 10 mM TRIS (pH 7.2), 1 mM EDTA and 20% sucrose (w/v), 1 mM DTT and protease inhibitors (we use "Complete, EDTA-free" tablets) at 4°C. Per 1 g fresh weight 2–3 ml buffer were used. All following working steps were done on ice at 4°C. The homogenate was cleared by spinning at 2,500 x g for five minutes at 4°C. The pellet was discarded and the supernatant was split into the cytosolic and microsomal fractions with spinning at 100,000 x g for 45 min at 4°C. The cytosolic supernatant was discarded and the microsomal pellet was resuspended in 2 ml TE-buffer for the sucrose density gradient or in 330/5 buffer (330 mM Sucrose, 5 mm potassium phosphate (pH 7.8) for the two-phase system.

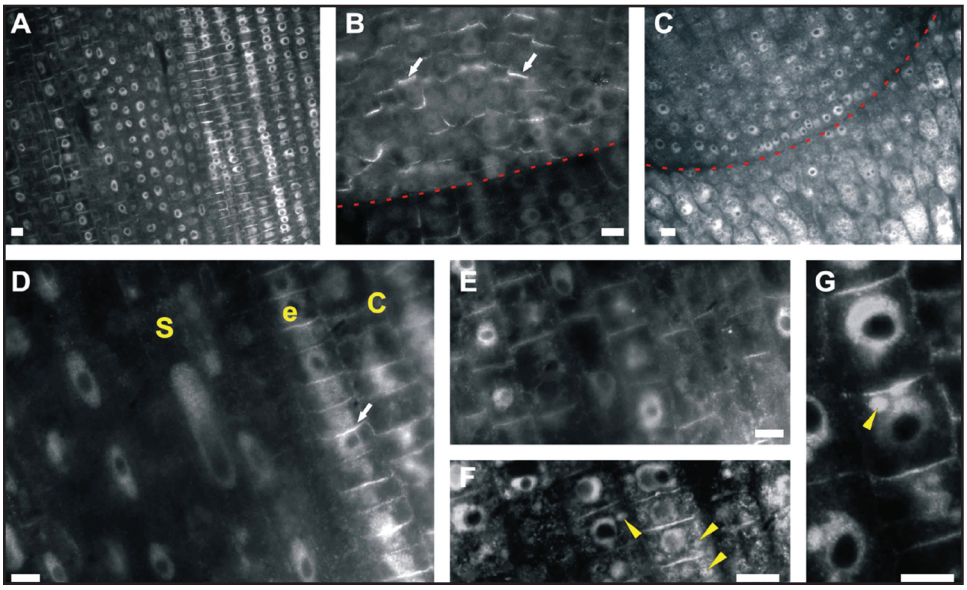

Figure 2. IAA labelings in maize root apices: subcellular and cellular distributions. (A, B) In the untreated root, IAA enriched cross-walls (end-poles) are prominent in stele cells of the transition zone (A) and the whole quiescent centre (QC) (B). (C, F and G) In BFA-treated root tips (2 h), IAA labeling of end-poles vanishes in the stele while the nuclear labelling gets more prominent. BFA treatment shifts IAA signal into BFA-induced compartments. (D) In cells of the cortex, intensity of the synapse labelling gets weaker while labelling of nuclei increases. White arrowheads point on auxin-enriched BFA-induced compartments. Red Line in (B) and (C) marks the border between meristem and root cap. (S, stele; e, endodermis; C, cortex) Bars: 10 μM.

Sucrose density gradient. From 20% to 60% sucrose in TE-buffer a step sucrose gradient was set up with five 2 ml steps. The resuspended microsomal fraction was laid over the gradient. The samples were spun for 18 hours in a SW41 swinging bucket rotor at 35,000 rpm at 4°C. Twelve 1 ml fractions were collected from the top of the gradient. The sucrose concentration in each fraction was measured by using a refractometer. In addition, the protein concentration of each fraction were measured with the method following Bradford.

Aqeous two-phase system. The aqueous two-phase partitioning method was done according to the batch procedure as described.[75] Phase separations were carried out in a series of 10-g phase systems with a final composition of 6.2% (w/w) dextran T500, 6.2% (w/w) polyethylene glycol 3350, 330 mM sucrose and 5 mm potassium phosphate (pH 7.8), 3 mm KCl and protease inhibitors. Three successive rounds of partitioning yielded the final upper phases and lower phases. The combined upper phase was enriched in plasma membranes vesicles and the lower phase contained intracellular membranes.

The final upper and lower phases were diluted 5- and 10-fold, respectively, in ice-cold Tris-HCl dilution buffer (10 mM, pH 7.4) containing 0.25 M Suc, 3 mM EDTA, 1 mM DTT, 3.6 mM l-Cys, 0.1 mM MgCl and the protease inhibitors. The fractions were centrifuged at 100,000 g for 60 min. The pellets were then resuspended in TE buffer and used for the protein concentration measured with the method following Bradford. All procedures were carried out at 4°C.

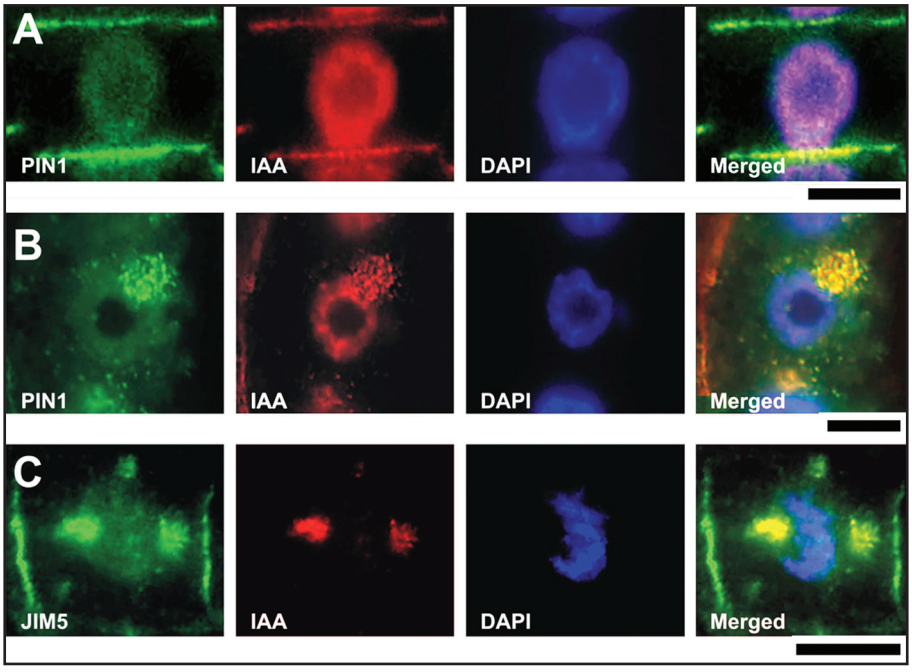

Figure 3. PIN1 and IAA colocalization in control and BFA-treated root apices. (A) In untreated roots, colocalization of PIN1 with IAA in distinct patches at the end-poles is obvious. (B and C) After 2 h of BFA exposure, PIN1, IAA, and JIM5-positive cell wall pectins colocalize in patch-like structures within endocytic BFA-induced compartments. Bars: 10 μM.

The samples were precipitated with methanol and chloroform. Five-hundred microliters of a fraction was combined with 500 μl MetOH and 125 μl chloroform in a eppendorf tube and vortexed. After centrifugation for ten minutes at 13.000 rpm at 4°C resulted in a two phased sample. The upper phase was discarded. After the addition of 500 μl MetOH, a second centrifugation of ten minutes with 13.000 rpm at 4°C was done. The resulting pellets had to dry completely and were resuspended in 1x SDS-PAGE sample buffer (final protein concentration of 1 μg per μl). Each sample was loaded onto an 15% SDS- PAGE gel which was blotted onto nitrocellulose.

All working steps of the immunoblotting were done at room temperature. The nitrocellulose was washed in TBS buffer (10 mM TRIS (pH 7.4), 150 mM NaCl) and then blocked with 4% BSA in TBS for one hour. After five minutes washing in TBS, incubation with the first antibodies (1:1000 or 1:2000) in TBS was carried out. The nitrocellulose was washed three times in TBS with 0,05% Tween 20 (TTBS) to get rid of unspecific antibody binding. The secondary antibodies are alkalic phosphatase conjugated and were used 1:10.000 in TBS. After one hour

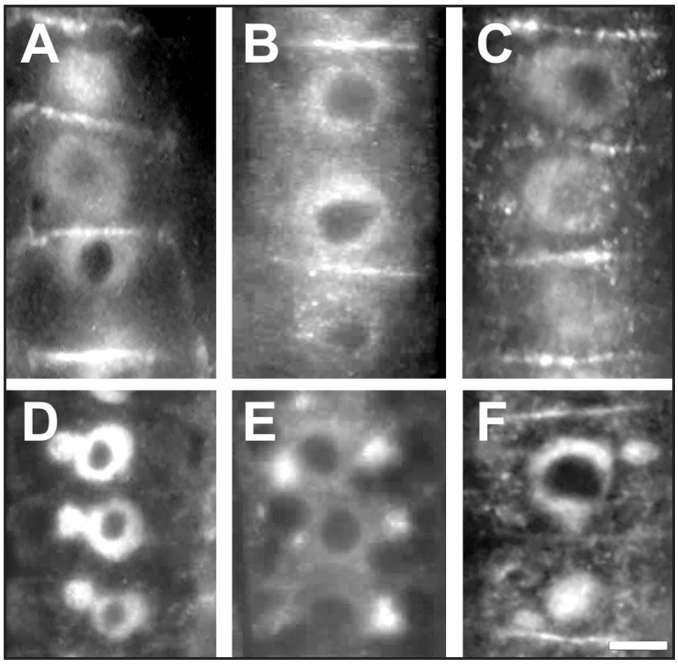

Figure 4. Comparison of IAA labelings at end-poles and within nuclei. (A) Control. (B) TIBA-treatment. (C) IAA-treatment. (D) Wild-type after the BFA treatment. (E) TIBA/BFA treatment. (F) IAA/BFA treatment. Bars: (A–C) and (F) 10 μM; (D and E) 8 μM.

incubation time, a washing with TTBS was repeated three times. The antibody detection was done with BCIP-NPT (Sigma Chemical). The staining was stopped with 1% acetic acid in water.

Real time recordings of auxin uptake into root apices. Real time recordings of auxin uptake into root cells with a vibrating microelectrode system was described in detail previously.[15]

Image processing and fluorescence measurements. Image processing was done with Photoshop 7 from Adobe and fluorescence measurement was done with the open source software Image-J (http://rsb.info.nih.gov/ij/).

RESULTS

Preparation and characterization of the IAA-specific antibody. IAA was coupled to BSA using the Mannich reaction.[36] The immunization schedule and purification of antibodies were done as described previously.[37,38] All immunized rabbits produced antisera to the IAA-N1-BSA conjugate, but serum titres and affinity of antibodies differed considerably and reflect differences in the responses of the individual animals. Therefore, the IAA antibody was well characterized in ELISA tests for several parameters (Table 1).

A number of structurally related indoles and IAA metabolites may be present in plant tissues. Antibody specificity is, therefore, a crucial point in the immunocytochemical assay of IAA. The compounds were tested for antibody binding over a range from 0.1 up to 50 nmol per assay. Data for auxins and related compounds producing zero molar cross-reactivities are not shown. Namely, IAA precursors such as tryptophan, tryptamine, tryptophol, indole-3-aldehyde, indole-3-acetonitrile, indole-3-acetamide were not reactive. All IAA conjugates were tested and shown to be inactive. IAA homologues like indole-3-acrylic acid and indole-3-propionic acid were weak competitors with cross-reactivity below 0.25%; significant immunoreaction was achieved only after using 500-times higher concentrations in plant tissues. Of the 25 compounds tested (Table 2), only α-naphthylacetic acid has relevant reactivity but this compound is a synthetic auxin and does not occur naturally.

Several controls were utilized in order to confirm the specificity of the IAA antibody at the level of immunolabeling: (1) labeling with the preimmune rabbit IgG instead of IAA antibody producing only black images (not shown), (2) labeling with the IAA antibody immunodepleted with an excess of IAA for 24 h (Fig. 1A), (3) labeling with the IAA antibody incubated with an excess of 2,4D, NAA and IBA for 24 h (Figs. 1B–D), (4) labeling only with the anti-rabit IgG, omitting the first antibody step producing only black images (not shown). Labelings with the IAA antibody of root apices treated with different concentrations of IAA show corresponding increases in the fluorescence signal (Fig. 1E). All these cytological controls unequivocally confirmed the specificity of the IAA antibody, as already documented at the biochemical level.

IAA immunolocalization in cells of control, BFA-, IAA- and TIBA-treated root apices. The localization of IAA in untreated maize roots showed that the most prominent signal was scored in cells of the root apex, especially in the transition zone (Fig. 2A) and in the quiescent centre (Fig. 2B). In these cells, a prominent auxin signal was visible at the cross-walls (end-poles), (Fig. 2A, D and E). In BFA-treated roots, IAA was still localized within nuclei while slightly weaker signal was scored at the end-poles (Fig. 2C, F and G). Additionally, BFA-induced compartments were enriched with auxin (Fig. 2G).

The signal at the end-poles was not a continuous labeling, but was composed of closely apposed spots at which IAA colocalized with PIN1 labeled with a maize specific PIN1-antibody (Fig. 3A). This colocalization was obvious also in BFA-treated cells when endocytic BFA-induced compartments were positive for PIN1 (Fig. 3B), IAA, as well as recycling cell wall pectins recognized by the JIM5 antibody (Fig. 3C). In control roots, all cell end-poles in the transition zone were enriched with auxin while nuclei were also labeled (Fig. 4A). In the TIBA treated roots, IAA was more enriched within nuclei while strong signal was scored also in the cytoplasm and at some end-poles (Fig. 4B and Suppl. Fig. 2). Exposure of root apices to external IAA resulted in increased signal in the cytoplasm when both nuclei and end-poles showed strong immunofluor-escence (Fig. 4C).

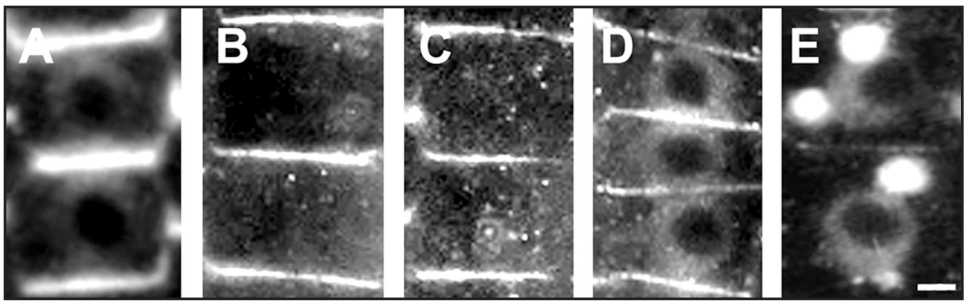

Figure 5. PIN1 labelings in cells of the transition zone of wild-type roots. (A) Control. (B) TIBA treatment. (C) TIBA/BFA treatment the combined treatments consisted of 2 hours of PAT inhibitor followed by two hours of BFA (D) BFA-treatment for ten minutes. (E) BFA-treatment for 2 hours. Bars: 10 μM.

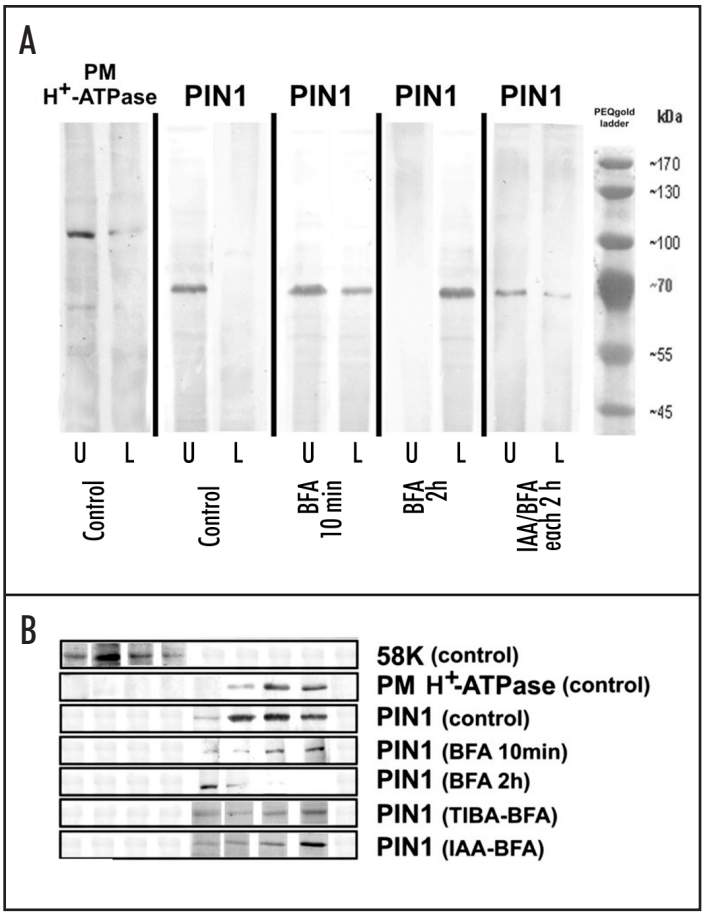

Figure 6. BFA shifts PIN1 from the plasma membrane to endosomes. (A) Aqueous Two-Phase System reveals that BFA induces shift of PIN1 from the plasma mebrane-enriched upper phase (U) into the endomembrane-enriched lower phase (L). Pretreatment with IAA inhibits this BFA-induced shift. (B) Sucrose density gradient analysis of PIN1 localization reveals that BFA induces shift of PIN1 from the plasma membrane into the endosomal fractions, but not to the Golgi apparatus fractions. Pretreatment with TIBA and IAA inhibits this BFA-induced shift. Comparison of treatments with fractions of matchable sucrose density. Sucrose density of fractions increases from left to right.

Importantly, BFA-treated wild-type roots showed IAA-enriched BFA-induced endocytic compartments (Fig. 4D). These compartments were smaller in TIBA and auxin pretreated roots (Fig. 4E and F).

BFA treatment shifts PIN1 from the plasma membrane into endosomes. PIN proteins show rapid vesicle recycling. We tested maize PIN1 antibody on western blots. The maize antibody shows one specific band around 70kDA (Fig. 6). Immunofluorescent labelings with the maize PIN1 antibody show that after two hours TIBA (for NPA and morphactins see supplemental Fig. 5) and after ten minutes BFA treatment, when auxin transport is inhibited, the PIN1 protein is still almost exclusively located at the plasma membrane at the apical cell pole (Figs. 5A–D). It is only after two hours duration of the BFA treatment that the PIN1 signal gets trapped within the BFA-induced compartments (Fig. 5E). Moreover, TIBA pretreatment prevents this accumulation of PIN1 within the endocytic BFA-induced compartments (Fig. 5C). Biochemical analysis using sucrose density gradients and aqueous two-phase system showed that PIN1 is strongly present at the plasma membrane after ten minutes BFA treatment. However, after two hours of BFA treatment, a shift from the PM protein fractions into endosomal protein fractions took place (Fig. 6). This shift can be prevented by TIBA and IAA pretreatments, both which are known to inhibit the endocytosis of PIN1 into *Arabidopsis* root cells.[7,11,12]

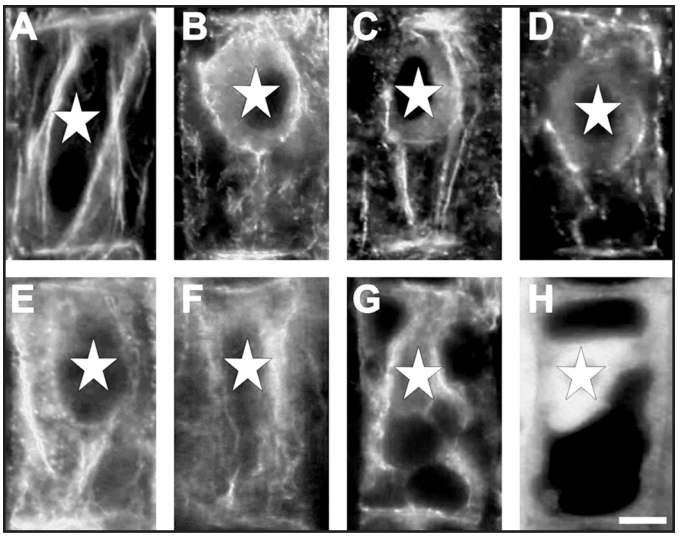

Figure 7. F-Actin arrangements in cells of the transition zone. (A) Control. (B) BFA treatment. (C) TIBA treatment. (D) NPA treatment. (E) Flurenol treatment. (F) Chlorflurenol treatment. (G) Chlorflurenolmethyl treatment. (H) Latrunculin B treatment. Note the depletion of F-actin from end-poles and disintegration of F-actin cables while nuclei are shifted from their original central position towards the basal cell pole. Bar: 8 μM.

BFA and different PAT inhibitors deplete F-actin from the end-poles. Next, we asked if the BFA-sensitive polarized secretion, based on endosomal vesicle recycling, is also related to the abundant F-actin at cell end-poles. BFA has an evident effect on these end-poles of the root apex cells when the typically abundant actin signal is weakened (Fig. 7A and B; see also ref. 31). Obviously, polarized secretion is essential to maintain the dense F-actin meshworks at end-poles. Interestingly, those tissues which accomplish PAT are also highly enriched in F-actin (Suppl. Fig. 1, see also ref. 39).

All the PAT inhibitors tested in this study, as well as latrunculin B, depleted F-actin at root end-poles and disintegrated the F-actin cables interconnecting the opposite end-poles and laterally contacting nuclear surfaces (Fig. 7A–H). Moreover, BFA and PAT-inhibitors induced a shift of nuclei towards the basal cell pole (Fig. 7B–G). Latrunculin B did not show this effect but induced accumulation of G-actin within nuclei (Fig. 7H).

In plants, similar to yeast and animal cells, F-actin assembly is promoted by molecules and membranes of the endocytic network.[32,40] An obvious question is, whether this F-actin depletion by PAT inhibitors is due to a generally lowered recycling of vesicles resulting from inhibited endocytosis.[7,11,12] To answer this question, we labeled cell wall pectins recycling between the plasma membrane—cell wall interface and endosomes.[16,41] Labelings after BFA-treatment showed that cell wall/endocytic pectins locate, like PIN molecules, within the BFA-induced endocytic compartments (Fig. 8). The size of these compartments reflects the recycling rate of cell wall pectins. Our data reveal that pretreatment with latrunculin B (Fig. 8F), as well as with all the PAT inhibitors tested, results in smaller BFA-induced compartments than those scored after BFA treatment alone (Fig. 8G, H and L–N).

Actin-enriched end-poles for PAT: Lessons from maize mutants. The maize mutant *semaphore1* is impaired in the negative regulation

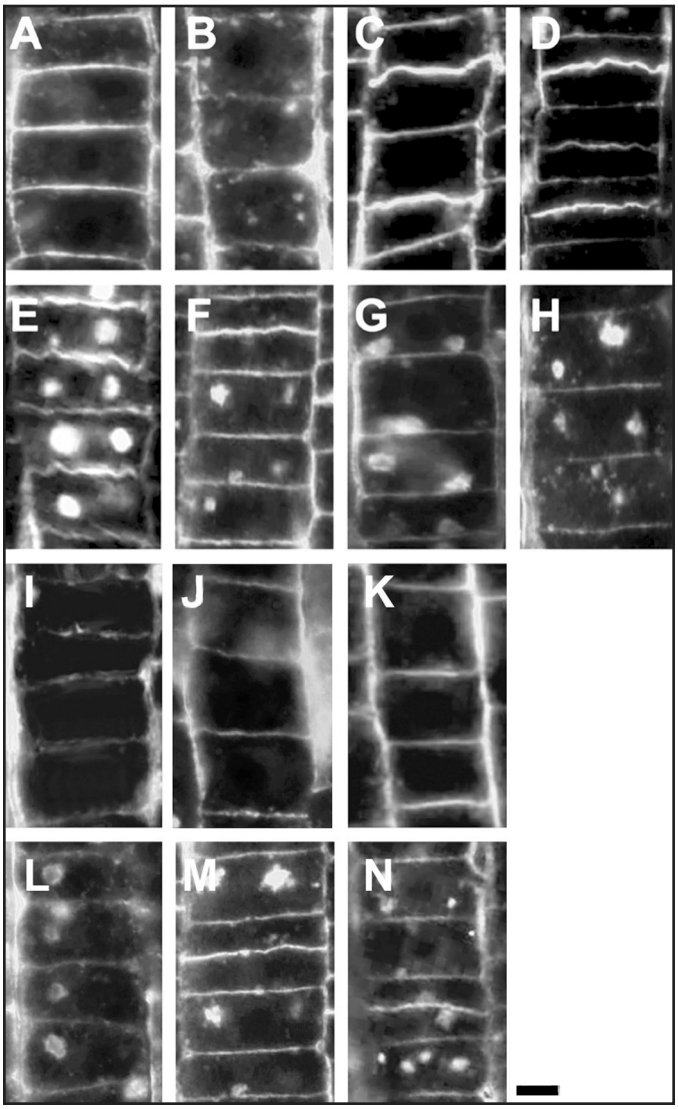

Figure 8. Labeling of the recycling pectin RGII in cells of the transition zone. (A) Control wild-type roots. (B) Latrunculin B-treated roots. (C) TIBA-treated roots. (D) NPA-treated roots. (E) BFA-treated roots. (F) Latrunculin B/BFA-treated roots. (G) TIBA/BFA-treated roots. (H) NPA/BFA-treated roots. (I) Flurenol-treated roots. (J) Chlorflurenol-treated roots. (K) Chlorflurenolmethyl-treated roots. (L) Flurenol/BFA-treated roots. (M) Chlorflurenol/BFA-treated roots. (N) Chlorflurenolmethyl/BFA-treated roots. Note that BFA-induced compartments are smaller in cells of roots pretreated with PAT inhibitors. All the treatments were for two hours, the combined treatments consisted of two hours of PAT inhibitors followed by two hours of BFA. Bar: 8 μM.

of KNOX1-genes and is characterized by reduced PAT, which is probably the reason for the pleiotropic phenotype of this mutant.[42] The root system of the mutant shows fewer lateral roots, a phenotype which is typical for a disturbed PAT.[43] Immunofluorescent labelings of root sections show that the polar cell organization of the mutant root is strongly disturbed. The actin cytoskeleton in cells of the transition zone shows changes which have strong similarity to those scored after treatments with diverse PAT inhibitors (Fig. 6). Moreover, actin and auxin fail to accumulate at the root end-poles in those mutants which are impaired in PAT (*semaphore1*, *rum1*, *rum1-lrt1*) but not in the *lrt 1* mutant[44] (Fig. 9) which shows normal auxin transport.[45] Exposure of *semaphore1* roots to BFA revealed that mutant cells have smaller BFA-induced compartments indicating decreased vesicular recycling rates (Fig. 9J). Moreover, while BFA-treated root cells of *rum1* and *lrt1-rum1* double mutant completely lacks any BFA- induced compartments (Fig. 9T and Y).

Similar depletion of F-actin from end-poles is also prominent in the maize mutant *rum1* and the *rum1-lrt1* double mutant (Fig. 9P and U). The *rum1* mutant is deficient in the initiation of seminal and lateral roots at the primary root.[45] Autoradiographic analysis also revealed that this mutant has also strongly reduced PAT in the root and, in accordance with this, no IAA-signal is detectable at the end-poles (Fig. 9Q). The *lrt1* mutant[44] shares some phenotypically similarities with the *rum1* mutant, including the missing initiation of lateral roots, has wild-type like PAT rates[46] and shows neither significant disturbances of the actin cytoskeleton nor the reduced IAA-Labelings at the end-poles (Fig. 9K and L). The double mutant *rum1-lrt1* shows a novel phenotype and has, like the *rum1*, a strongly reduced PAT.[45] The labelings are showing reduced F-actin and no detectable IAA at the end-poles (Fig. 9U and V). Importantly, PIN1 still localizes to the root end-poles of those mutants which are impaired in PAT (Fig. 9H, R and W) while auxin accumulates at the end-poles only when PAT is intact (Fig. 9B and L), but fails to accumulate there when PAT is reduced (Fig. 9G, Q and V).

In conclusion, after disturbances to the vesicle recycling, irrespective if induced by block to the polarized secretion by BFA or by prevention of the endocytosic via PAT inhibitors, the root cells show typical disintegration and depletion of the actin cytoskeleton at the root end-poles.

Real-time recordings of auxin uptake into wild-type and mutant root apices. In order to get information on auxin transport in living roots, we have taken advantage of the vibrating microelectrode system which allows continuous recordings of auxin fluxes in growing root apices of both maize and *Arabidopsis*.[15,46] This technique revealed that polar auxin flow is the most prominent in the distal portion of the transition zone and can be fully inhibited with classical auxin transport inhibitors NPA, TIBA, but also with BFA treatment.[15] Moreover, this technique reveals that the MDR-like ABC transporter, AtPGP4, is important for auxin transport[46] in this special root apex zone. Here we show that in the maize mutants *semaphore1*, *rum1* and *rum1-lrt1*, auxin influx is impaired particularly in this root region (Fig. 10).

DISCUSSION

The classical chemiosmotic concept (Fig. 11) can not explain the rapid PAT inhibition induced by Brefeldin A (BFA) within a few min,[14,15,28] when putative auxin transporters are still at the plasma membrane.[12] Moreover, this popular concept ignores also vacuoles and endosomes as possible compartments participating in PAT. Published papers do not critically address these issues and the classical chemiosmotic concept has remained unchallenged. Here we have embarked on a reinvestigation of several key aspects of PAT using a new auxin antibody, Steedman's wax embedding technique and recently characterized maize mutants impaired in PAT. We have obtained four types of observations which are incompatible with the classical chemiosmotic concept of PAT and are proposing an updated version of this concept (Fig. 11). This includes endosomes and vesicle recycling as essential parts of PAT, supporting a neurotransmitter-like secretory nature of auxin export. First of all, auxin is enriched within endosomes and at the auxin transporting end-poles of cells active in PAT, but not in cells impaired in PAT either due to PAT inhibitors or genetic lesions. Next, in maize mutants affected in PAT, PIN1 localizes abundantly to the end-poles but auxin and

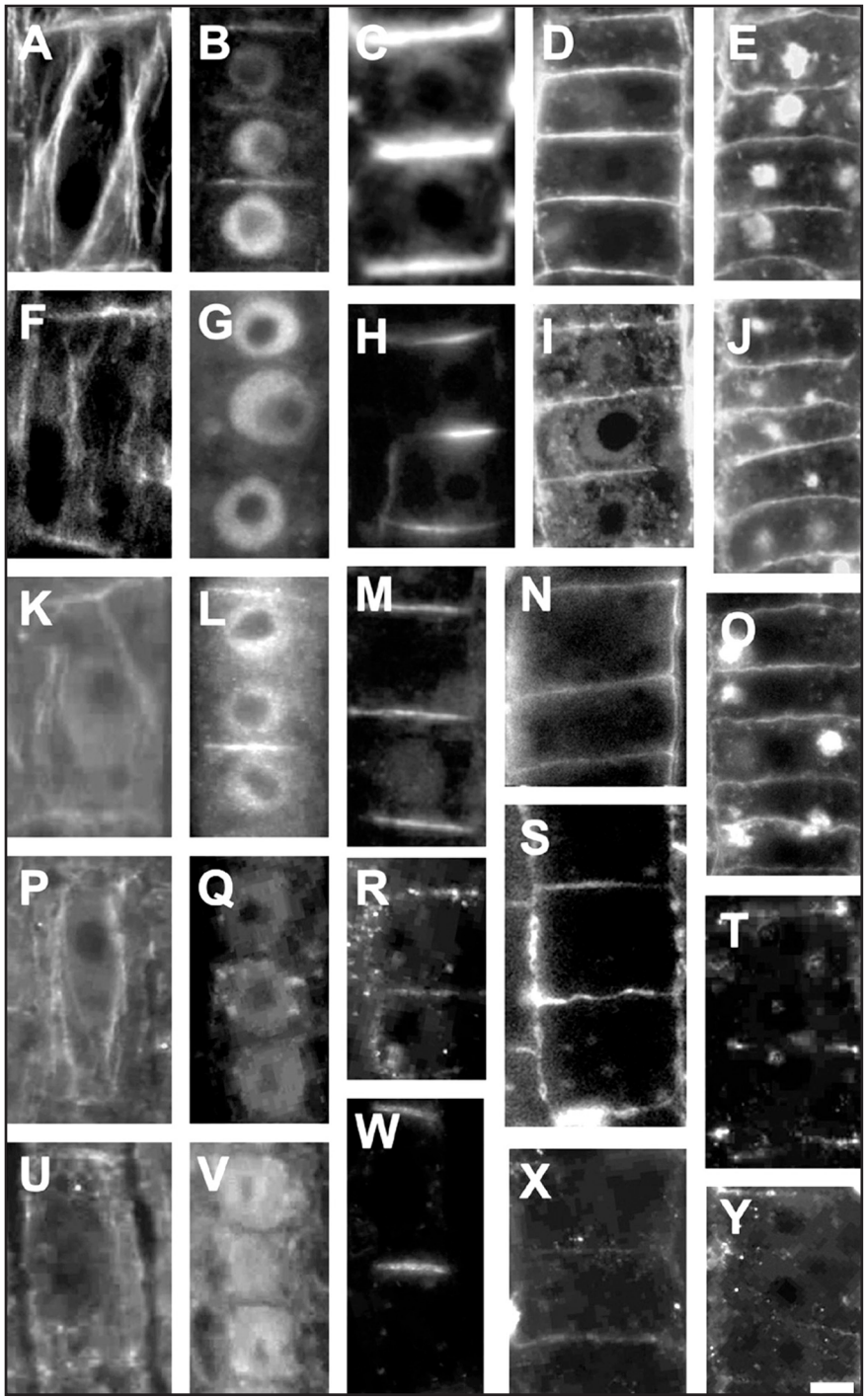

Figure 9. Actin, IAA, PIN1, and RGII labelings in root apices of wild-type and maize mutants. Actin (A, F, K, P, U), IAA (B, G, L, Q, V), PIN1 (C, H, M, R, W), and RGII (D, I, N, S, X) and RGII after two hours of BFA-treatment (E, J, O, T, Y) labelings in stele periphery cells of the transition zone the wild-type (A–E), *semaphore1* (F–J), *lrt1* (K–O), *rum1* (P–T), and *lrt1/rum1* (U–Y) mutants. Note the depletion of F-actin and IAA from the cellular end-poles, which is correlated with small size of BFA-induced compartments (E, J, O, T, Y) but PIN1 shows still a signal on the end-poles. The only exeption is the *lrt1* mutant which is, in contrast to all other mutants, also not affected in PAT.[44] Bars: A,C,F,K, N, P, S, U and X, 8 μM; B, D, E, G, H, I, J, L, M, O, Q, R, T, V,W and Y, 10 μM.

F-actin is depleted from the end-poles which also fail to support the formation of large BFA-induced compartments. In addition, biochemical analysis confirmed earlier cytological data that PIN1 is still at the plasma membrane after 10 minutes of BFA treatment, when auxin efflux is already strongly inhibited.[14,28] Last but not least, three classes of PAT inhibitors (TIBA, NPA, morphactins), differing chemically, all deplete F-actin from the end-poles and inhibit endocytosis/vesicle recycling.

Direct localization of IAA, using our new specific antibody, in cells of the root apex of maize failed to reveal the previously reported auxin maximum in cells of the quiescent centre and root cap statocytes, as was shown with the DR5 promoter line of *Arabidopsis*.[3,19,20,47] This finding is not so unexpected, because other auxin reporters visualize 'auxin maximum' at other locations. For instance, the BA3 construct visualizes an 'auxin maxima' in those cells which are embarking on rapid cell elongation[22-24] (Suppl. Fig. 3). These conflicting observations indicate that these reporters just reflect particular signaling cascades feeding into the activation of these auxin-responsive transcription promoters. There are also several other problems associated with auxin- response reporters.[48] All this makes it more-and-more obvious that, in order to understand the nature of processes driving PAT, we need to localize auxin directly using specific antibodies. Unfortunately, those antibodies which are available and currently in use recognize auxin as well as auxin conjugates.[27] Here we are introducing a newly generated antibody which is monospecific for IAA and does not recognize IAA conjugates.

Our data show, that a prominent cell compartment in the maize root tissue, which accumulates auxin, is the nucleus. This is not surprising, particularly with regard to the auxin-responsive elements discussed above, but especially because of the nuclear auxin receptor TIR1 which is active in its auxin-bound form within nuclei, activating transcription of auxin-regulated genes.[49,50] Besides nuclei, we have identified the actin-enriched end-poles and adjacent endosomal compartments as auxin enriched domains in maize roots. This finding has far-reaching consequences for the field of auxin research. Cellular end-poles,[51] conceptually characterized as "plant synapses",[29,33] emerge as subcellular domains specialized for the transcellular transport of auxin along cell files. The currently popular version of the chemiosmotic theory is considering only the auxin pools which are localized within the pH neutral cytoplasm and the acidic cell wall compartment (apoplast, for recent reviews and dispatches, refs. 4, 5, 52, 53). This assumption ignores any possible contribution of acidic endosomes for the maintenance and regulation of PAT. Our immunofluorescence data on auxin localization reveal that auxin is accumulated within endosomes, which communicate with the auxin-transporting end-poles[29,33] and get aggregated into BFA-induced compartments. Importantly, these auxin-enriched endosomes may represent the elusive BFA-sensitive source of auxin from which auxin is secreted out of cells via BFA-sensitive processes.[29] Auxin accumulating endosomes may also act as putative 'auxin vacuum

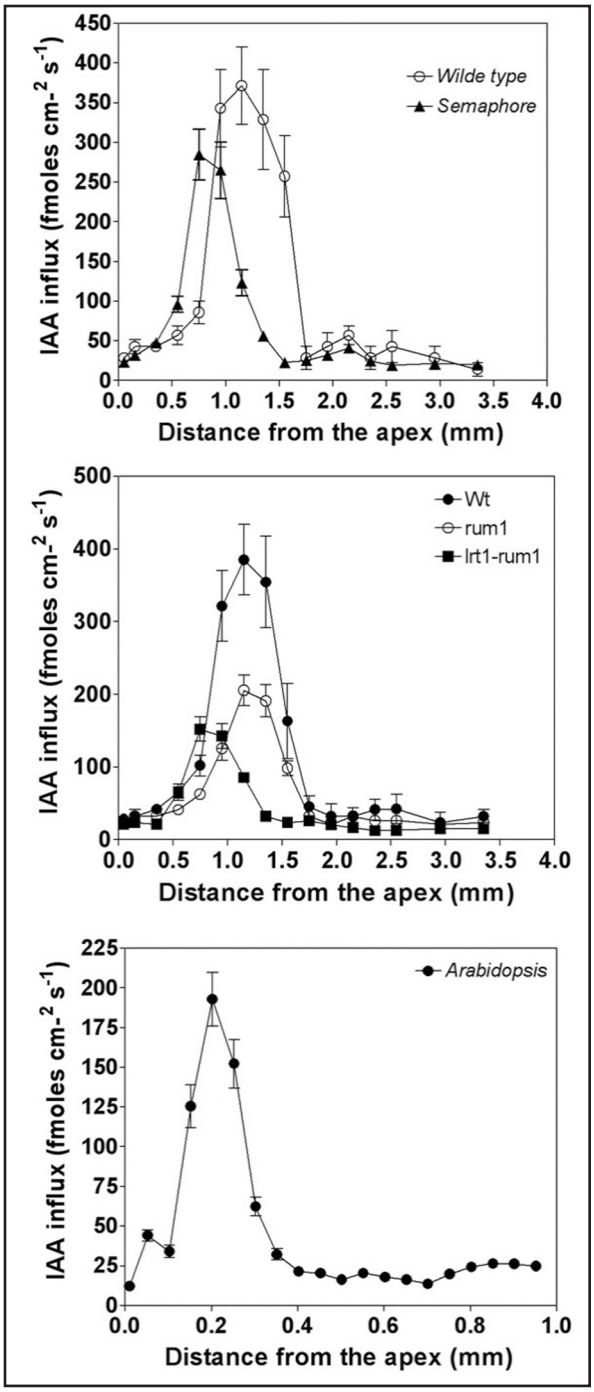

Figure 10. Real-time recordings of auxin uptake into wild-type and, mutant roots. Auxin uptake (transport) shows peak in the distal part of the transition zone (1.0–1.5 mm form the root apex junction). All mutants show a highly reduced auxin influx in this particular root zone, but not in cells of the elongation region. For more information on this technique, see reference 15.

cleaners'[30,54] which would effectively remove all free auxin from orifices of plasmodesmata in order to prevent their 'uncontrolled' diffusion from cell-to-cell. This function of auxin-accumulating endosomes would be particularly important during early embryogenesis, when plasmodesmata are known to allow free passage of signaling molecules, hormones and peptides, demonstrating that all embryonic cells are part of a single syncytium (symplast).[34,35] Free and uncontrolled passage of auxin within this syncytium would be incompatible with the intricate local and polar auxin accumulations in early embryos.[3]

Cells of the root apex transition zone are unique also with respect to the actin organization. They assemble F-actin enriched plasma membrane domains at the end-poles, which serve as dynamic platforms for rapid endocytosis and high rate of vesicle recycling. Those tissues, which are active in PAT, such as the stelar cells accomplishing acropetal PAT and the cells of the epidermis and outer cortex driving basipetal PAT, are enriched in F-actin[29,30,33,39] (Suppl. Fig. 1). Particularly, F-actin is prominent at the end-poles accomplishing abundant vesicle recycling.[29,30,33] This allows effective cell-cell communication based on synaptic processes as we know them from neuronal and immunological synapses.[29,30,33,55] For instance, auxin that has been secreted into the end-pole cell wall (cross-wall) space, has been reported to elicit electric responses in the adjacent cells (reviewed in ref. 55). All this indicates that auxin acts, in addition to its hormonal and morphogen-like properties, as a neurotransmitter-like agent.[4,29] Other puzzling data also fall in the right place. For instance, the rapid blockage of PAT after cold exposure,[56,57] which is also known to block endocytosis in root cells,[16] and almost immediate recovery of PAT after returning the plants to room temperature.[56,57] For example, the finding that synaptic proteins occur in plants, like the Arabidopsis protein BIG which is present in plant and animal genomes. This protein, which has similarity to the synaptic protein CALLOSIN/ PUSHOVER driving synaptic signal transmission at neuromuscular synapses, is essential for PAT in plants[12,58] and its action is related to endocytosis and vesicle recycling at plant end-poles acting as plant synapses.[29,33] Another puzzling observation is also making sense now, namely that extracellular auxin inhibits endocytosis, and the activity of BIG is important for this unexpected auxin action.[12] BIG is relevant also for the endosomal BFA-sensitive secretion, because *lpr1* mutant, which is allelic to *BIG*, is phenocopied by treatment of wild-type seedlings with BFA.[58]

Obviously, the classical chemiosmotic model has difficulties to explain the rapid blockage of the auxin export out of cells after inhibition of vesicular secretion with BFA and monensin.[12-15,28] Furthermore, it can not explain rapid inhibition of PAT after cold exposure[56,57] and with inhibitors of actin polymerization.[60,61] Delbarre et al. (1998)[28] reported that auxin efflux from plant cells is blocked with agents affecting proton gradients and intracellular pH status. The latter authors interpreted these data only from the perspective of the classical chemiosmotic theory. However, these findings appear in a new perspective if we consider the accumulation of auxin within endosomes of root cells. Intriguingly, the activity of H^+-pyrophosphatase AVP1 is involved in PAT[59] and this further supports our concept of neurotransmitter-like secretion, via secretory endosomes, as the major pathway for exporting auxin ut of plant cells.[4,29,33] Present data, supporting the neurotransmitter-like concept of PAT, explain why the activity of H^+-pyrophosphatase AVP1 drives PAT in *Arabidopsis* roots.[59] Pyrophosphatases represent single-subunit H^+ pumps, which generate an electrochemical gradient across delimiting membranes of small vacuoles and endosomes.[62,63] Overexpression of AVP1 stimulates PAT, while *avp1-1* null mutants show a reduction of PAT.[61] Moreover, overexpression of AVP1 stimulates root growth,[61,64] while null mutants have severely disrupted roots.[61] In addition to the vacuolar membrane, the AVP1 signal was found at punctated structures and, importantly, discontinuous sucrose gradient analysis revealed association of AVP1 with the endosomal fraction.[61] It is not easy to explain all these observations with the classical chemiosmotic concept. The *Perspectives Science* article,[65]

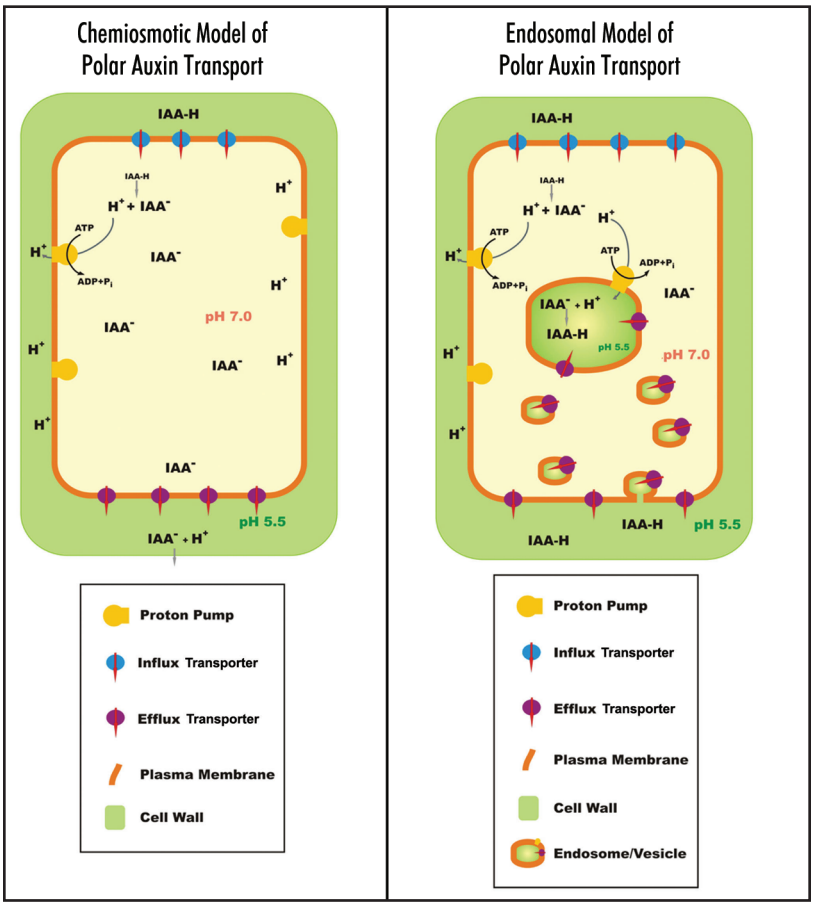

Figure 11. Schematical comparison of the classical chemiosmotic and the updated endosomal models for the PAT. The most important difference between the models is the involvement of endosomes in both accumulation and regulated secretion of IAA out of exporting cells. Note that the endosomal interior is topologically part of the cell's exterior. This is also consistent with respect to low pH values and endosomal enrichments with cell wall pectins.[16,17,32,41]

commenting this paper,[59] suggested that AVP1 acidifies the putative X compartment.[65] This corresponds nicely to the auxin-enriched endosomes reported in our paper and summarized in our model (Fig. 11).

Interestingly in this respect, VHA-a1 subunit of the vacuolar ATPase (V-ATPase) which acidifies endosomes, vacuoles and the trans-Golgi network in plant cells, localizes to the plant early endocytic compartments in root cells of *Arabidopsis*.[66] It will be important in the future to analyze PAT in the available V-ATPases mutants in *Arabidopsis*. The dwarf phenotype of the *det3* mutant (c subunit) due to lack of cell elongation[67] indicates that PAT requires both PPase[59] and V-ATPase activities. Moreover, VHA-a1 subunit of the V-ATPase colocalizes with TGN SNAREs[67] and one of these (VTI1) is essential for the basipetal PAT.[68] Intriguingly, PM-based PIN1 localizes properly in the polar manner,[68] despite strongly affected PAT in the VTI1 mutant, resembling the situation reported in the present study for maize mutants affected in PAT. The acidic nature of auxin and of endosomes implies that auxin relies on the continuous activity of putative vesicular transporters in order to be enriched within endosomes. The vesicular nature of PIN2 was strongly indicated by a recent study using yeast and HeLa cells.[69] Mutation by changing Serine97 to glycine resulted only in vesicular localization of PIN2 in yeast cells which accumulated auxin.[69] Interpreting these data, it is important to keep in mind that the endosomal interior is de facto the extracellular space. So transporting auxin into the endosomal interior with PIN2 efflux protein removes it from the cytoplasm.

Taken together, there is an urgent need for an update of the classical chemiosmotic model for PAT (Fig. 11). Besides acidic cell walls and neutral cytoplasm, acidic endosomes emerge as a new important player in the transcellular pathway of auxin transport. Importantly, regulated secretion out of cells, via secretory endosomes, would then accomplish presumably a quantal efflux of protonated auxin into the extracellular space. From there, it can either freely diffuse back to the same cell or into adjacent cells. In addition, adjacent cells could also import auxin through the activities of putative auxin transporters at the plasma membrane and/or via endocytosis of auxin molecules embedded within cell wall material like pectins and hemicelluloses. In accordance with this latter notion, it has been shown that the internalization of these cell wall molecules is particularly active at the auxin transporting end-poles.[16,17,32,33,66] The 'synaptic' nature[29,33] of these end-poles has been strongly supported recently by showing that PIN1 localization to these sub-cellular domains is dependent on the cell-cell contacts.[8] As soon as these adhesive contacts are lost, due to a long-term absence of microtubules, PIN1 rapidly redistributed from these domains to the whole plasma membrane.[8] Future studies should focus on both endosomes and regulated vesicular recycling in order to unravel critical details of the polar transport of auxin across cellular boundaries in plant tissues.

Acknowledgements

We thank J. Friml for the DR5::GFP line and Y. Oono for the BA3::GUS line. We also thank Liam Dolan for the JIM5 antibody, Toru Matoh for the RGII antibody and Wolfgang Michalke for the PM-H$^+$ATPase antibody. Financial support by grants from the Deutsches Zentrum für Luft und Raumfahrt (DLR, Cologne, Germany; project 50WB 0434), from the European Space Agency (ESA-ESTEC Noordwijk, The Netherlands; MAP project AO-99-098) and from the EC Research Training Networks (Brussels, Belgium; project TIPNET HPRN-CT-2002-00265) is gratefully acknowledged. F.B. receives partial support from the Slovak Academy of Sciences (Grant Ageny VEGA, Bratislava, Slovakia; project 2/5085/25) and M.S. receives support by grant MSM6198969216.

References

1. Swarup R, Bennett M. Auxin transport: The fountain of life in plants? Dev Cell 2003; 5:824-6.
2. Bhalerao RP, Bennett MJ. The case for morphogens in plants. Nat Cell Biol 2003; 5:939-943.
3. Friml J, Vieten A, Sauer M, Weijers D, Schwarz H, Hamann T, Offringa R, Jürgens G. Efflux-dependent auxin gradients establish the apical-basal axis of *Arabidopsis*. Nature 2003; 426:147-53.
4. Friml J, Wisniewska J. Auxin as an intercellular signal. In: Flemming A, ed. Intercellular Communication in Plants. Annual Plant Reviews 16, Blackwell Publishing, 2005.
5. Leyser O. Auxin distribution and plant pattern formation: How many angels can dance on the point of PIN? Cell 2005; 121:819-22.
6. Paponov IA, Teale WT, Trebar M, Blilou I, Palme K. The PIN auxin efflux facilitators: Evolutionary and functional perspectives. Trends Plant Sci 2005; 10:170-7.
7. Geldner N, Anders N, Wolters H, Keicher J, Kornberger W, Muller P, Delbarre A, Ueda T, Nakano A, Jürgens G. The *Arabidopsis* GNOM ARF-GEF mediates endosomal recycling, auxin transport, and auxin-dependent plant growth. Cell 2003; 112:219-30.

8. Boutté Y, Crosnier MT, Carraro N, Traas J, Satiat-Jeunemaitre B. The plasma membrane recycling pathway and cell polarity in plants: Studies on PIN proteins. J Cell Sci 2006; 119:1255-65.
9. Schneider G. Morphactins: Physiology and performance. Annu Rev Plant Physiol 1970; 21:499-536.
10. Katekaar JF, Geissler AE. Auxin transport inhibitors. IV. Evidence of a common mode of action for a proposed class of auxin transport inhibitors. Plant Physiol 1980; 66:1190-5.
11. Geldner N, Friml J, Stierfhoff Y, Jürgens G, Palme K. Auxin transport inhibitors block PIN1 cycling and vesicle trafficking. Nature 2001; 413:425-8.
12. Paciorek T, Zazímalová E, Ruthhardt N, Petrásek J, Stierhof YD, Kleine-Vehn J, Morris DA, Emans N, Jürgens G, Geldner N, Friml J. Auxin inhibits endocytosis and promotes its own efflux from cells. Nature 2005; 435:1251-6.
13. Wilkinson S, Morris DA. Targeting of auxin carriers to the plasma membrane: Effects of monensin on transmembrane auxin transport in *Cucurbita pepo* L. tissue. Planta 1994; 193:194-202.
14. Delbarre A, Muller P, Imhoff Y, Guern J. Comparison of mechanisms controlling uptake and accumulation of 2,4-dichlorophenoxy acetic acid, naphthalene-1-acetic acid, and indole-3-acetic acid in suspension-cultured tobacco cells. Planta 1996; 198:532-41.
15. Mancuso S, Marras AM, Volker M, Baluska F. Noninvasive and continuous recordings of auxin fluxes in intact root apex with a carbon-nanotube-modified and self-referencing microelectrode. Anal Biochem 2005; 341:344-51.
16. Baluska F, Hlavacka A, Samaj J, Palme K, Robinson DG, Matoh T, McCurdy DW, Menzel D, Volkmann D. F-actin-dependent endocytosis of cell wall pectins in meristematic root cells: Insights from brefeldin A-induced compartments. Plant Physiol 2002; 130:422-31.
17. Samaj J, Baluska F, Voigt B, Schlicht M, Volkmann D, Menzel D. Endocytosis, actin cytoskeleton and signalling. Plant Physiol 2004; 135:1150-61.
18. Aloni R, Schwalm K, Langhans M, Ullrich C. Gradual shifts in sites of free-auxin production during leaf-primordium development and their role in vascular differentiation and leaf morphogenesis. Planta 2003; 216:841-53.
19. Sabatini S, Beis D, Wolkenfelt H, Murfett J, Guilfoyle T, Malamy J, Benfey P, Leyser O, Bechtold N, Weisbeek P, Scheres B. An auxin-dependent distal organizer of pattern and polarity in the *Arabidopsis* root. Cell 1999; 99:463-72.
20. Friml J, Benková E, Blilou I, Wisniewska J, Hamann T, Ljung K, Woody S, Sandberg G, Scheres B, Jürgens G, Palme K. AtPIN4 mediates sink-driven auxin gradients and root patterning in *Arabidopsis*. Cell 2002; 108:661-73.
21. Blilou I, Xu J, Wildwater M, Willemsen V, Paponov I, Friml J, Heidstra R, Aida M, Palme K, Scheres B. The PIN auxin efflux facilitator network controls growth and patterning in *Arabidopsis* roots. Nature 2005; 433:39-44.
22. Oono Y, Chen QG, Overvoorde PJ, Köhler C, Theologis A. Age mutants of *Arabidopsis* exhibit altered *auxin*-regulated gene expression. Plant Cell 1998; 10:1649-62.
23. Armstrong JI, Yuan S, Dale JM, Tanner VN, Theologis A. Identification of inhibitors of auxin transcriptional activation by means of chemical genetics in *Arabidopsis*. Proc Natl Acad Sci USA 2004; 101:14978-83.
24. Ramírez-Chávez E, López-Bucio J, Herrera-Estrella L, Molina-Torres J. Alkamides isolated from plants promote growth and alter root development in *Arabidopsis*. Plant Physiol 2004; 134:1058-68.
25. Nakamura A, Higuchi K, Goda H, Fujiwara MT, Sawa S. Brassinolide induces *IAA5*, *IAA19*, and DR5, a synthetic auxin response element in *Arabidopsis* implying a cross-talk point of brassinosteroid and auxin signaling. Plant Physiol 2003; 133:1-11.
26. Nemhauser JL, Mockler TC, Chory J. Interdependency of brassinosteroid and auxin signaling in *Arabidopsis*. PLOS Biol 2004; 2:1460-71.
27. Aloni R, Aloni E, Langhans M, Ullrich C. Role of auxin in regulating *Arabidopsis* flower development. Planta 2005; 223:315-28.
28. Delbarre A, Muller P, Guern J. Short-lived and phosphorylated proteins contribute to carrier-mediated efflux, but not to influx, of auxin in suspension-cultured tobacco cells. Plant Physiol 1998; 116:833-44.
29. Baluska F, Samaj J, Menzel D. Polar transport of auxin: Carrier-mediated flux across the plasma membrane or neurotransmitter-like secretion? Trends Cell Biol 2003; 13:282-5.
30. Baluska F, Hlavacka A. Plant formins come to age: Something special about cross-walls. New Phytol 2005; 168:499-503.
31. Paciorek T, Friml J. Auxin signaling. J Cell Sci 2006; 119:1199-202.
32. Samaj J, Read ND, Volkmann D, Menzel D, Baluska F. The endocytic network in plants. Trends Cell Biol 2005; 15:425-33.
33. Baluska F, Volkmann D, Menzel D. Plant synapses: Actin-based adhesion domains for cell-to-cell communication. Trends Plant Sci 2005; 10:106-11.
34. Stadler R, Lauterbach C, Sauer N. Cell-to-cell movement of green fluorescent protein reveals post-phloem transport in the outer integument and identifies symplastic domains in *Arabidopsis* seeds and embryos. Plant Physiol 2005; 139:701-12.
35. Kim I, Cho E, Crawford K, Hempel FD, Zambryski PC. Cell-to-cell movement of GFP during embryogenesis and early seedling development in *Arabidopsis*. Proc Natl Acad Sci USA 2005; 102:2227-31.
36. Pengelly W, Meins F. A specific radioimmunoassay for nanogram quantities of the auxin, indole-3-acetic acid. Planta 1977; 136:173-80.
37. Dewitte W, Chiappetta A, Azmi A, Witters E, Strnad M, Rembur J, Noin M, Chriqui D, Van Onckelen H. Dynamics of cytokinins in apical shoot meristems of a day-neutral tobacco during floral transition and flower formation. Plant Physiol 1999; 199:111-22.
38. Pence VC, Caruso JL. ELISHA determination of IAA using antibodies against ring-linked IAA. Phytochemistry 1987; 26:1251-5.
39. Baluska F, Vitha S, Barlow PW, Volkmann D. Rearrangements of F-actin arrays in growing cells of intact maize root apex tissues: A major developmental switch occurs in the postmitotic transition region. Eur J Cell Biol 1997; 72:113-21.
40. Samaj J, Baluska F, Voigt B, Volkmann D, Menzel D. Endocytosis and actomyosin cytoskeleton. In: Samaj J, Baluska F, Menzel D, eds. Plant Endocytosis. Springer Verlag, 2005.
41. Baluska F, Liners F, Hlavacka A, Schlicht M, Van Cutsem P, McCurdy D, Menzel D. Cell wall pectins and xyloglucans are internalized into dividing root cells and accumulate within cell plates during cytokinesis. Protoplasma 2005; 225:141-55.
42. Scanlon MJ, Henderson DC, Bernstein B. *SEMAPHORE1* functions during the regulation of ancestrally duplicated *knox* genes and polar auxin transport in maize. Development 2002; 129:2663-73.
43. Casimiro I, Beeckman T, Graham N, Bhalerao R, Zhang H, Casero P, Sandberg G, Bennett MJ. Dissecting *Arabidopsis* lateral root development. Trends Plant Sci 2003; 8:165-71.
44. Hochholdinger F, Feix G. Early post-embryonic root formation is specifically affected in the maize mutant *lrt1*. Plant J 1998; 16:247-55.
45. Woll K, Borsuk LA, Stransky H, Nettleton D, Schnable PS, Hochholdinger F. Isolation, characterization, and pericycle-specific transcriptome analyses of the novel maize lateral and seminal root initiation mutant *rum1*. Plant Physiol 2005; 139:1255-67.
46. Santelia D, Vincenzetti V, Azzarello E, Bovet L, Fukao Y, Düchtig P, Mancuso S, Martinoia E, Geisler M. MDR-like ABC transporter AtPGP4 is involved in auxin-mediated lateral root and root hair development. FEBS Lett 2005; 579:5399-406.
47. Ottenschläger I, Wolff P, Wolverton C, Bhalerao RP, Sandberg G, Ishikawa H, Evans M, Palme K. Gravity-regulated differential auxin transport from columella to lateral root cap cells. Proc Natl Acad Sci USA 2003; 100:2987-91.
48. Jenik PD, Barton MK. Surge and destroy: The role of auxin in plant embryogenesis. Development 2005; 132:3577-85.
49. Dharmasiri N, Dharmasiri S, Weijers D, Lechner E, Yamada M, Hobbie L, Ehrismann JS, Jürgens G, Estelle M. Plant development is regulated by a family of auxin receptor F box proteins. Dev Cell 2005; 9:109-19.
50. Parry G, Estelle M. Auxin receptors: A new role for F-box proteins. Curr Opin Cell Biol 2006; 18:152-6.
51. Baluska F, Wojtaszek P, Volkmann D, Barlow PW. The architecture of polarized cell growth: The unique status of elongating plant cells. BioEssays 2003; 25:569-76.
52. Moore I. Gravitropism: Lateral thinking in auxin transport. Curr Biol 2002; 12:R452-5.
53. Blakeslee J, Peer WA, Murphy AS. Auxin transport. Curr Opin Cell Biol 2005; 8:494-500.
54. Samaj J, Chaffey NJ, Tirlapur U, Jasik J, Volkmann D, Menzel D, Baluska F. Actin and myosin VIII in plasmodesmata cell-cell channels. In: Baluska F, Volkmann D, Barlow PW, eds. Cell-Cell Channels. Landes Bioscience and Springer Verlag, 2006.
55. Baluska F, Mancuso S, Volkmann D, Barlow PW. Root apices as plant command centres: The unique 'brain-like' status of the root apex transition zone. Biologia 2004; 59:9-17.
56. Wyatt S, Rashotte A, Shipp M, Robertson D, Muday G. Mutations in the gravity persistence signal loci in *Arabidopsis* disrupts the perception and/or signal transduction of gravitropic stimuli. Plant Physiol 130:1426-35.
57. Nadella V, Shipp MJ, Muday GK, Wyatt SE. Evidence for altered polar and lateral auxin transport in the *gravity persistent signal* (*gps*) mutants of Arabidopsis. Plant Cell Environm 2006; 29:682-90.
58. López-Bucio J, Hernández-Abreu E, Sánchez-Calderón L, Pérez-Torres A, Rampey RA, Bartel B, Herrera-Estrella L. An auxin transport independent pathway is involved in phosphate stress-induced root architectural alterations in *Arabidopsis*. Identification of *BIG* as a mediator of auxin in pericycle cell activation. Plant Physiol 2005; 137:681-91.
59. Hu S, Brady SR, Kovar D, Staiger CJ, Clarke GB, Roux SJ, Muday G. Identification of plant F-actin-binding proteins by F-actin chromatography. Plant J 2000; 24:127-37.
60. Sun H, Basu S, Brady SR, Luciano RL, Muday GK. Interactions between auxin transport and the actin cytoskeleton in developmental polarity of *Fucus distichus* embryos in response to light and gravity. Plant Physiol 2004; 135:266-78.
61. Li J, Yang H, Peer WA, Richter G, Blakeslee JJ, Bandyopadhyay A, Titapiwatanakun B, Undurraga S, Khodakovskaya M, Richards EL, Krizek B, Murphy AS, Gilroy S, Gaxiola R. *Arabidopsis* H^+-PPase AVP1 regulates auxin-mediated organ development. Science 2005; 310:121-5.
62. Rea PA, Poole RJ. Vacuolar H^+-translocating pyrophosphatase. Annu Rev Plant Physiol Plant Mol Biol 1999; 44:157-80.
63. Ratajczak R, Hinz G, Robinson DG. Localization of pyrophosphatase in membranes of cauliflower inflorescence cells. Planta 1999; 208:205-11.
64. Park S, Li J, Pittman JK, Berkowitz GA, Yang H, Undurraga S, Morris J, Hirschi KD, Gaxiola RA. Up-regulation of a H^+-pyrophosphatase (H^+-PPase) as a strategy to engineer drought-resistant crop plants. Proc Natl Acad Sci USA 2005; 102:18830-5.
65. Grebe M. Growth by auxin: When a weed needs acid. Science 2005; 310:60-1.
66. Dettmer J, Hong-Hermesdorf A, Stierhof YD, Schumacher K. Vacuolar H^+-ATPase activity is required for endocytic and secretory trafficking in *Arabidopsis*. Plant Cell 2006; 18:715-30.
67. Schumacher K, Vafeados D, McCarthy M, Sze H, Wilkins T, Chory J. The *Arabidopsis det3* mutant reveals a central role for the vacuolar H^+-ATPase in plant growth and development. Genes Dev 1999; 13:3259-79.

68. Surpin M, Zheng H, Morita MT, Saito C, Avila E, Blakeslee JJ, Bandyopadhyay A, Kovaleva V, Carter D, Murphy A, Tasaka M. The VTI family of SNARE proteins is necessary for plant viability and mediates different protein transport pathways. Plant Cell 2003; 15:2885-99.
69. Petrasek J, Mravec J, Bouchard R, Blakeslee JJ, Abas M, Seifertova D, Wisniewska J, Tadele Z, Kubes M, Covanova M, Dhonukshe P, Skupa P, Benkova E, Perry L, Krecek P, Lee OR, Fink GR, Geisler M, Murphy AS, Luschnig C, Zazimalova E, Friml J. PIN proteins perform a rate-limiting function in cellular auxin efflux. Science 2006; 312:914-8.
70. Strnad M, Vanek T, Binarová P, Kamínek M, Hanus J. Enzyme immunoassays for cytokinins and their use for immunodetection of cytokinins in alfalfa cell culture. In: Kutácek M, Elliott MC, Macháckova I, eds. Molecular Aspects of Hormonal Regulation of Plant Development. The Hague: SPB Academic Publ., 1990:41-54.
71. Strnad M, Veres K, Hanus J, Siglerová V. Immunological methods for quantification and identification of cytokinins. In: Kamínek M, Mok DWS, Zazímalová E, eds. Physiology and Biochemistry of Cytokinins in Plants. The Hague: SPB Academic Publ, 1992:437-446.
72. Strnad M, Peters W, Beck E, Kamínek M. Immunodetection and identification of N6-(o-hydroxybenzylamino)purine as a naturally occurring cytokinin in *Populus x canadensis* Moench cv. Robusta leaves. Plant Physiol 1992; 99:74-80.
73. Harlow E, Lane D. Antibodies - A laboratory manual. USA: Cold Spring Harbor Laboratory, 1998.
74. Weiler EW, Jourdan PS, Conrad W. Levels of indole-3-acetic acid in intact and decapitated coleoptiles as determined by a specific and sensitive solid-phase enzyme immunoassay. Planta 1981; 153:561-71.
75. Larsson C, Widell S, Kjellbom P. Preparation of high-purity plasma membranes. Methods Enzymol 1987; 148:558-68.